Acceleron Aerospace Journal || AAJ.11.2106-2456
Volume 3, Issue 4, pp (545-552)
Review Paper
E-ISSN- 2583-9942 || DOI: 10.61359/11.2106-2456

EMI Shielding Materials in Drones

Aparna A. R[*], Shamanth PV[†], Adrian J. Fernandes[‡], B. S. Janani[§], Chaithra G[**]

Dhruv Bhansali[††], Divya Shri Raju[‡‡], Natin Kumar[§§]

Department of Aerospace Engineering, B.M.S. College of Engineering, Bangalore, India – 560019

Abstract: The rapid advancement of UAV technology has increased system complexity, particularly in cellular network applications where UAVs work alongside ground-based base stations. A major challenge is electromagnetic interference (EMI) in the radiofrequency (RF) band, caused by components such as motors and power supplies, which can disrupt communication signals. Effective shielding is crucial to ensure uninterrupted UAV operation, as external EMI from base stations can jeopardize UAV electronics, leading to unintended flight paths or loss of communication. This review explores enhanced security measures for UAV electronics in RF environments, proposing three materials for EMI shielding: reduced graphene oxide (RGO), electrically conductive epoxy resins filled with polyaniline (PANI) and polypyrrole (PPy), and hybrid polymer composites using a polyvinylidene fluoride (PVDF) matrix with few-layer graphene (FLG) and nickel spinel ferrites (NSF).

Table of Contents

1. Introduction

An unmanned aerial vehicle (UAV), or drone, is an aircraft operated without a human pilot, crew, or passengers on board. Originally developed throughout the 20th century for military operations deemed too "dull, dirty, or dangerous" for human involvement, UAVs became vital military tools by the 21st century. With advancements in control technologies and decreasing costs, UAVs found widespread use beyond military contexts. Their applications now include aerial photography, area surveillance, precision agriculture, forest fire monitoring, river and environmental monitoring, policing, infrastructure inspections, smuggling, product deliveries, entertainment, and drone racing. According to Roman Kubacki et al. [2], a typical drone is built with a non-metallic frame that serves as its structural backbone. The propellers are attached to rotors connected to engines powered by batteries, which are regulated by voltage controllers. A key element of every drone is the Internal Measurement Unit (IMU), which includes an accelerometer, gyroscope, and barometer. More advanced models may also feature a compass and GPS module. Electromagnetic interference (EMI) refers to disruptions in an electrical circuit caused by external sources. These disturbances can stem from both natural events, such as lightning, and human-made sources, like powered audio equipment or speakers. EMI can lead to malfunctions or complete failures of electronic devices. Roman Kubacki et al. [2] suggest that a simple countermeasure against such radiation is to cover the drone's exterior with a microwave absorber. This approach is particularly crucial for UAVs, as their electromagnetically permeable shells offer minimal protection against incoming RF radiation. Ideal absorbers should provide high shielding effectiveness (SE) across a wide frequency range while also being lightweight to prevent adding undue weight to the UAV and weather-resistant to withstand environmental conditions.

[*]UG Research Scholar, Department of Aerospace Engineering, B.M.S. College of Engineering, Bangalore, India – 560019.
[†] UG Research Scholar, Department of Aerospace Engineering, B.M.S. College of Engineering, Bangalore, India – 560019.
[‡] UG Research Scholar, Department of Aerospace Engineering, B.M.S. College of Engineering, Bangalore, India – 560019.
[§] UG Research Scholar, Department of Aerospace Engineering, B.M.S. College of Engineering, Bangalore, India – 560019.
[**] UG Research Scholar, Department of Aerospace Engineering, B.M.S. College of Engineering, Bangalore, India – 560019.
[††]UG Research Scholar, Department of Aerospace Engineering, B.M.S. College of Engineering, Bangalore, India – 560019.
[‡‡]UG Research Scholar, Department of Aerospace Engineering, B.M.S. College of Engineering, Bangalore, India – 560019.
[§§] UG Research Scholar, Department of Aerospace Engineering, B.M.S. College of Engineering, Bangalore, India – 560019.
Corresponding Author: abhiamith12@gmail.com.
****** Received: 16-September-2024 || Revised: 28-September-2024 || Accepted: 30-September-2024 || Published Online: 30-September-2024.

This paper discusses the aspects of reduced graphene oxide (RGO) as one of the promising materials for use as a microwave absorber. We selected unmodified RGO due to its lightweight nature, being one of the lightest graphene derivatives, as well as its relatively low production cost. The investigation highlights RGO's electrical properties, identifying it as an efficient absorber, particularly suited for UAV applications. The major point of comparison with other materials is based on the shielding performance across various frequencies. RGO's shielding effectiveness under free-space conditions, assuming the transparency of the drone housing, provides insights into its reflective and absorptive properties. EMI shielding should be integrated into the structural composite materials, utilizing conductive fillers such as carbon fibers or fabrics commonly used in aircraft manufacturing. Recent advancements in EMI shielding materials involve intrinsically conductive polymers (ICPs) like polyaniline (PANI), polypyrrole (PPy), polythiophene (PTh), and poly(3,4-ethylenedioxythiophene) (PEDOT). These polymers address issues related to weight and corrosion resistance, offering enhanced lightness, processability, and tunability of shielding performance. Modern developments often combine ICPs with conductive particle fillers, such as PPy with nickel particles, PPy with multi-walled carbon nanotubes (MWCNT) and silver particles, PANI with barium ferrite and expanded graphite, and PANI with ceramic particles. These innovations have broadened the frequency range and improved the tunability of EMI shielding materials, as confirmed by various studies.

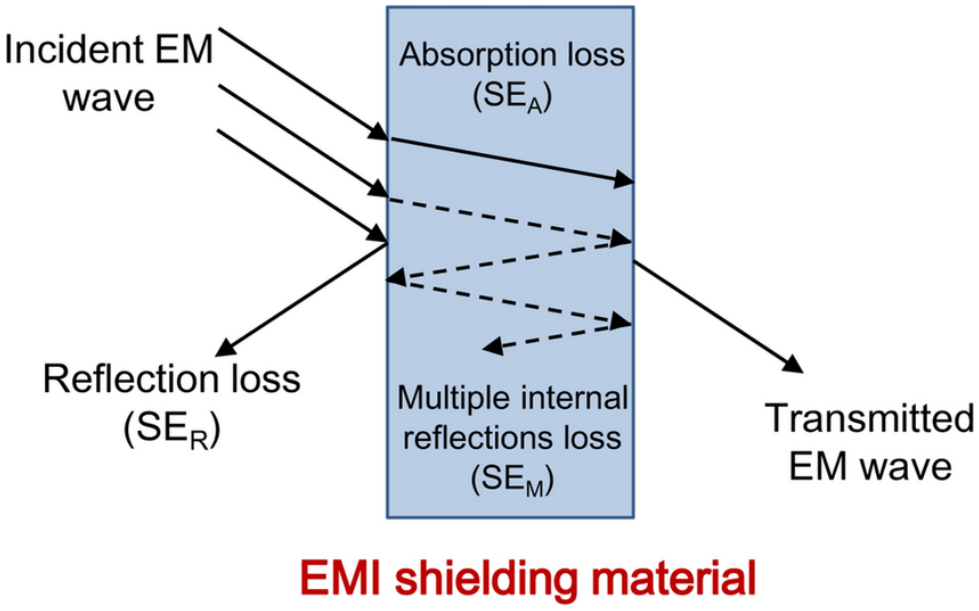

Figure-1 Electromagnetic interference shielding [11]

Carbonaceous and ferritic fillers are highly valued for their ability to interact with electromagnetic (EM) waves, attenuating the electric and magnetic components, respectively. Current trends focus on hybrid composites, incorporating both carbonaceous and ferritic nanofillers into polymer matrices. While carbon nanotubes (CNTs) have been widely used, graphene has gained popularity due to its cost-effectiveness and similar properties. There is increasing interest in combining graphene with other fillers, such as CNTs and ferrites, to enhance the electromagnetic interference (EMI) shielding of polymer nanocomposites (PNCs). Upcoming studies have examined shielding effectiveness in a frequency range of 0.1 – 10 GHz.

2. Materials

2.1. Reduced Graphene Oxide (RGO)

2.1.1 Method 1

Roman Kubacki et al. [2] synthesized Graphene Oxide (GO) by oxidizing graphite powder (53 µm, 10 grams) using a modified Hummer's method. The graphite powder was mixed with 230 mL of concentrated sulfuric acid in a beaker and cooled in an ice bath. After adding 30 grams of KMnO4 and 300 mL of deionized water (DM), the mixture was stirred at 35°C for 2 hours and left for 5 days. Subsequently, 500 mL of DM

water and 25 mL of H2O2 were added, and the suspension was filtered and washed with 1 L of a 1:9 HCl solution, followed by DM water until neutral pH was achieved. The suspension was sonicated for 30 minutes at 40 kHz, centrifuged at 4000 rpm for 30 minutes, and dried in an oven at 70°C for 20 hours.

Reduced Graphene Oxide (RGO) can be synthesized using two methods: microwave-assisted reduction and hydrothermal reduction. For microwave-assisted synthesis, 0.15 grams of GO was dissolved in 50 mL of DM water, sonicated for 1 hour, and adjusted to pH 11 with NH3. The solution was heated in a microwave at 1000 watts for 8 minutes, then filtered, washed with ethanol, and dried at 110°C for 6 hours. In the hydrothermal reduction method, 1 gram of GO was stirred in 100 mL of ethanol for 30 minutes, transferred to a Teflon-lined autoclave, and heated at 200°C for 10 hours. The product was filtered, washed with DM water, and dried at 70°C for 6 hours before further processing and characterization.

Both GO and RGO are successfully synthesized from graphite. The synthesis of GO is performed using the modified Hummer's method. In this study, the synthesis of RGO through hydrothermal heating is found to be more effective than microwave heating.

2.1.2 Method 2

For the preparation of reduced graphene oxide (RGO), 400 mg of graphene oxide (GO) was dispersed in 400 mL of water via ultrasonic treatment for 30 minutes, forming a homogeneous brown suspension. The pH was adjusted to 10 using ammonia, followed by the addition of hydrazine hydrate with a weight ratio of 10:7 (hydrazine hydrate to GO). The mixture was heated at 80°C for 24 hours, resulting in the precipitation of a black substance. The product was filtered, washed with methanol and water, and dried at 80°C for 24 hours.

RGO was prepared with the aid of $NH_3 \cdot H_2O$ aqueous and hydrazine hydrate successfully. The characterization results indicate that the layer spacing of graphite oxide was longer than that of graphite. The crystal structure of graphite was changed **[7]**.

With the use of RGO as an absorber, the level of the RF environment can be effectively reduced to the safe level. The safe level, at frequencies emitted by mobile base stations, can be obtained using an even thin layer of 3 mm. In this case, the level of radiation penetrating through the housing of the device is 3.4 V/m at 3.6 GHz and 0.6 V/m at 5.8 GHz. With a thicker layer, it can be much better.

At 5 mm thickness, the RGO material with a pure structure has a shielding effectiveness (SE) of 10 to 59 decibels at frequencies of 0.1 to 10 GHz **[7]**.

At 3 mm thickness, the RGO material with a pure structure has a shielding effectiveness (SE) of 8 to 40 decibels at frequencies of 0.1 to 10 GHz.

2.2 Hybrid Polymer Composites using FLG and NSF

In the study by Ibrar Ahmed et al. **[4]**, hybrid polymer composites are prepared using few-layer graphene (sourced from XG Sciences), PVDF pellets with a molecular weight of 180,000 (purchased from Sigma Aldrich), and synthesized nickel spinel ferrites (NSF). The NSF is synthesized via a chemical reaction route, starting with nickel and iron nitrates in salt form. These salts are dissolved separately in distilled water at concentrations of 0.1 M and 0.2 M, and then combined at a temperature of 80–85°C. A second solution (3 M) is prepared by adding sodium hydroxide (NaOH) dropwise over 60 minutes as the temperature reaches 80–85°C. The resulting mixture is washed multiple times to achieve a neutral pH of 7.0. The precipitates are dried and calcined in an electric furnace at 850°C for 6 hours, followed by crushing and grinding in a mortar.

The polymer composites are fabricated using the solution casting method. The three components—PVDF (50 mg/ml), FLG (5 mg/ml), and NSF (10 mg/ml)—are each dissolved in DMF. The samples are prepared with varying weight ratios as outlined in Table 1.

Table-1 Polymer Composite Samples

PVDF	PVDF 100 wt%
PVDF/FLG-3	PVDF 97 wt%/FLG 3 wt%
PVDF/FLG-3/NSF-15	PVDF 82 wt%/FLG 3 wt%/NSF 15 wt%
PVDF/FLG-3/NSF-30	PVDF 67 wt%/FLG 3 wt%/NSF 30 wt%

To disperse the few-layer graphene (FLG), the solution is magnetically stirred for 24 hours and then ultrasonicated for 30 minutes. Nickel spinel ferrites (NSF) are then added, and the mixture is mechanically stirred for 4 hours. The resulting solution is poured into petri dishes and dried in a vacuum oven at 80°C under a pressure of 300 mbar. The dried films are subsequently used for characterization.

For morphological analysis, a scanning electron microscope (SEM, JOEL JSM-6490A) is employed. SEM images of the fractured surfaces of the composite films (fractured using liquid nitrogen) are examined to study their microstructure. Figure 2 presents representative SEM images, displaying the morphology of neat PVDF (a) and the hybrid composites (b–c). Proper dispersion of the fillers within the polymer is crucial, especially for the targeted application of electromagnetic interference (EMI) shielding, which relies on the formation of a network structure for optimal performance. The fillers appear to be uniformly dispersed across all samples, promoting the formation of an electrically conductive network.

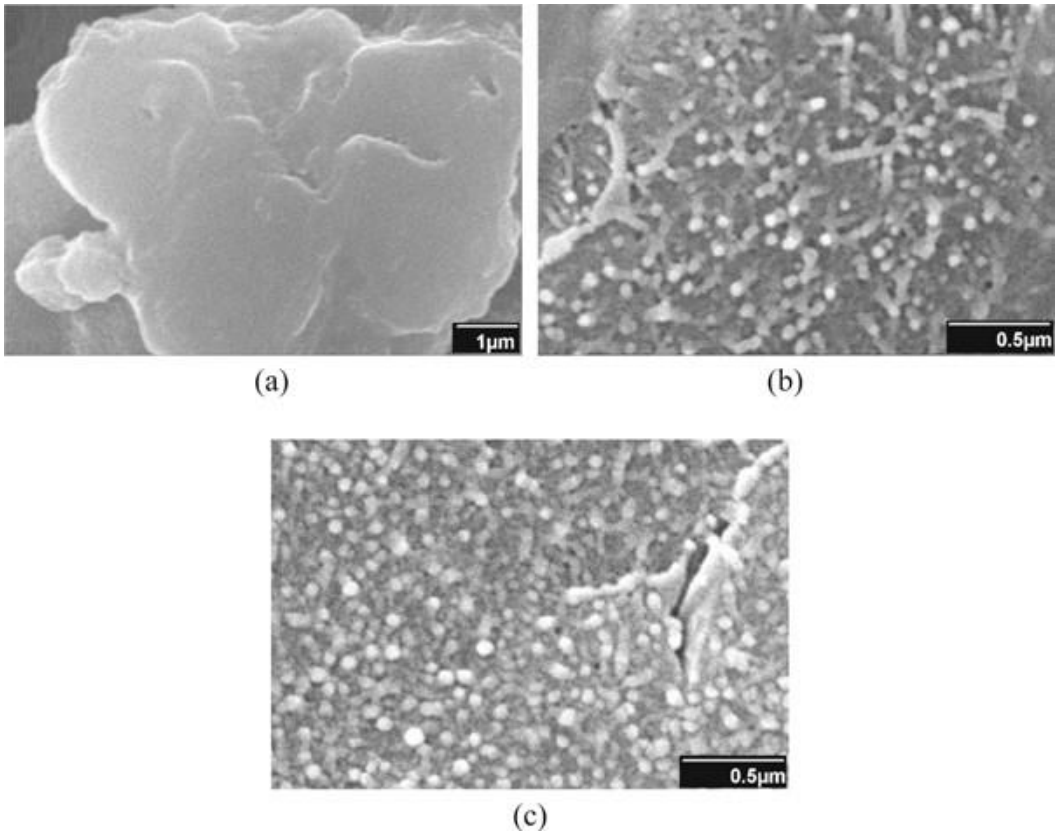

Figure-2: Representative SEM images of (a) neat PVDF (b) PVDF/FLG-3/NSF-15 (c) PVDF/FLG-3/NSF-30 [4]

Hybrid polymer composites based on few-layer graphene nanosheets and nickel spinel ferrites have been prepared for EMI shielding applications in the 1–12 GHz frequency range. Both fillers, few-layer graphene and nickel spinel ferrites, significantly enhanced the shielding effectiveness of the polymer composites, achieving ~45 dB and a maximum of ~53 dB for PVDF/FLG-3 and PVDF/FLG-3/NSF-15, respectively. The interfacial interaction may also contribute to the enhanced absorption of EM waves. However, further increasing the ferritic

content (30 wt%) resulted in compromised shielding effectiveness compared to the aforementioned samples, mainly due to aggregation issues. Additionally, the shielding effectiveness depends on material thickness—the thicker the material, the better the shielding effectiveness. The only downside of thicker materials is that they can cause an excessive increase in overall weight.

2.3 Electrically Conductive Epoxy Resins Filled with Polyaniline (PANI) And Poly Pyrrole (Ppy)

2.3.1 Preparation of Epoxy/PANI Composite

To prepare the epoxy resin composites with PANI, various concentrations of PANI (0%, 10%, 15%, 20%, and 30% by weight) were mixed into the epoxy resin [5]. The mixture was homogenized using a sonication bath for 2 hours to ensure uniform dispersion of PANI within the resin. After homogenization, a hardener was added, and the composite was cast onto a glass plate. The composite was cured at room temperature for 24 hours and then post-cured in an oven at 120°C. A schematic of the process is shown in Figure 3.

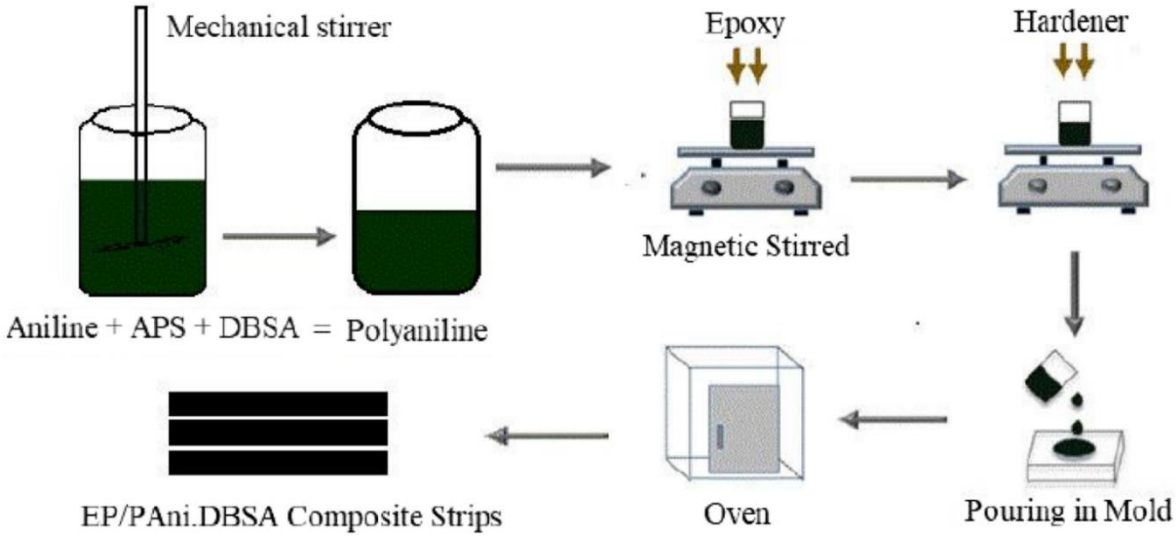

Figure-3: Schematic of conductive composites preparation. [5]

2.3.2 Characterization

- **FTIR Spectroscopy:** The FTIR spectra of pure PANI and the epoxy/PANI composites were recorded using the FTIR-4100 system over a wavenumber range of 500–4000 cm^{-1}.
- **Mechanical Testing:** A universal testing machine (ZWICK ROLL Z100) was used to measure the mechanical properties of the composites.
- **Electrical Conductivity:** The electrical conductivity of the prepared samples was measured at room temperature using the four-probe method with a Keithley 2450. A four-probe station with tungsten probes (26 mm length, 45° cone angle, 25 µm tip radius, and 1 mm spacing) was employed. A schematic for the conductivity measurement is shown in Figure 4.

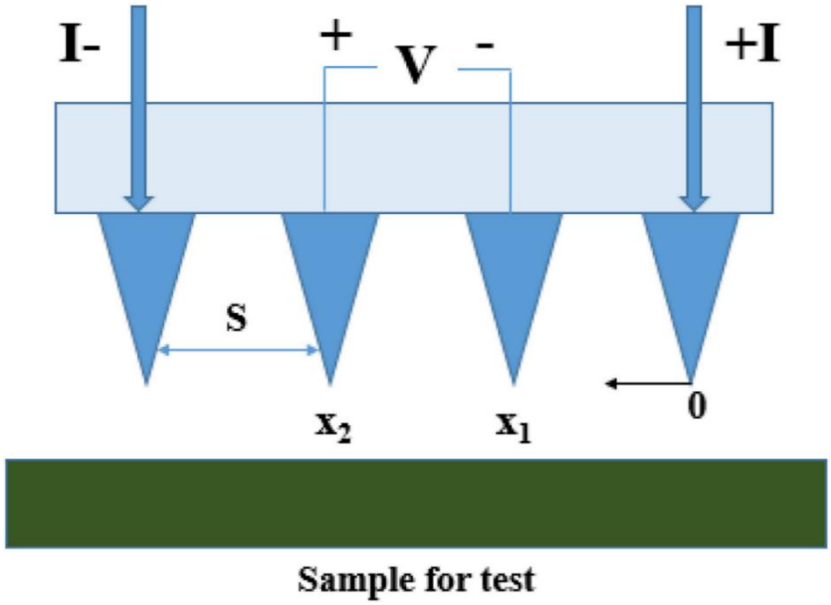

Figure=4: Probe dimensions and positioning for rectangular sample. [5]

2.3.3 Equation

$$\sigma = V \cdot AI \cdot L$$

Where:

- V = applied voltage,
- I = current,
- R = resistance,
- L = length,
- A = area,
- σ = DC conductivity.

EMI Shielding and NIR Characterization:

- **EMI Shielding:** The effectiveness of EMI shielding was measured over a microwave frequency range of 0.1 GHz to 20 GHz using the VNA technique. A sample with an outer diameter of 13 mm and a thickness of 2.5 mm was tested.
- **NIR Measurements:** The NIR spectra (700 nm–2500 nm) were obtained using Perkin Elmer's Lambda 950 equipment.

2.3.4 Morphological Analysis

- **SEM Imaging:** SEM was used to analyze the fractured surface of the composite films. The films were frozen in liquid nitrogen and then broken to expose the unaltered cross-sectional area for high-magnification imaging.
- **Zeta Sizer Analysis:** The particle size of PANI nanoparticles was measured using Malvern's Zeta Sizer AT, which is capable of detecting particles between 1 nm and 1000 nm with an accuracy of ±2%. A 0.5 wt% PANI nanoparticle solution in water was prepared for particle size determination.

Conductive epoxy/PANI composites were successfully prepared using a physical mixing process. The conductive filler was homogenized using an ultrasonic bath. The mechanical and electrical properties were found to vary with the PANI content. A 20 wt% PANI concentration yielded optimal electromechanical

properties, with a tensile modulus of 81.28 MPa, a tensile strength of 42 MPa, and a conductivity of 1.3×10^{-15} S/cm. As the PANI content increased, the conductivity improved, reaching 3.51×10^{-13} S/cm at 30 wt%, though mechanical properties deteriorated due to incomplete curing. The composites demonstrated effective EMI shielding, with 63 dB of shielding effectiveness (SE) and less than 0.5% NIR transmission in the entire NIR region **[8]**.

2.3.1 Preparation of Epoxy/PANI Composite

Step 1: Preparation of PPy Nanospheres (NSs)

The synthesis of PPy nanospheres involved the use of pyrrole (Py), ammonium persulfate (APS), and para-toluene sulfonic acid (PTSA) in a 6:3:5 molar ratio. Solution 1 consisted of PTSA (60 mmol) and APS (36 mmol) dissolved in 400 mL of deionized water, sonicated in an ice-water bath for 1 hour. Solution 2 was prepared by dissolving pyrrole (72 mmol) in 100 mL of deionized water. Solution 2 was slowly added to Solution 1 and sonicated for an additional hour. The product was vacuum filtered, washed with ethanol and deionized water, and dried at 50 °C overnight.

Step 2: Preparation of PPy Nanofibers (NFs)

A sol-gel of V_2O_5 (1 mL) was prepared and introduced into 60 mL of 1 M HCl, followed by the addition of 1 mL of pyrrole monomer. APS (1.15 g) was added as an oxidant, and the solution was stirred for 2 hours. The process of vacuum filtration was used to obtain bulk PPy nanofibers, which were then washed and dried at 80 °C overnight.

Step 3: Preparation of PPy/Epoxy Nanocomposites

Epoxy resin composites with 1.0, 5.0, 10.0, and 20.0 wt% of PPy nanofibers and nanospheres were the output of this preparation. PPy nanostructures were immersed in epoxy resin overnight, then mechanically stirred at 600 rpm for 1 hour. A curing agent was added in a monomer/curing agent ratio of 100/26.5, followed by further stirring. The mixture was degassed at 70 °C and cured at 120 °C for 5 hours. Finally, the temperature of the nanocomposites was brought down to room temperature.

PPy nanocomposites were successfully synthesized and analyzed. The rheological behavior indicated pseudoplasticity, while 1.0 wt% PPy nanofibers improved the tensile strength of the composite by 29%, reaching 90.36 MPa. Increasing PPy content led to enhanced flame retardancy and dielectric properties, with stronger interfacial polarization observed in nanofiber composites. Both PPy nanofibers and nanospheres contributed to improved mechanical, dielectric, and flame-retardant properties in the nanocomposites **[8]**.

PANI and PPy are advantageous materials for use in the manufacturing of construction materials due to their commercial availability, low costs, and high conductivities. The fabrication routes described in this study led to the formation of polymer grains in the form of nanoparticles (PPy) and microfibers (PANI), which are expected to increase the adhesion and compatibility between conducting polymer fillers and epoxy resin. Therefore, the fabrication of the resulting composite material is a simple and economic process, devoid of the necessity to employ advanced manufacturing technologies. The optimal content of ICPs in epoxy resin based on PANI and PPy is approximately 30 vol%. The composites manufactured using these two conducting polymers with carbon fiber reinforcement were subjected to electromagnetic compatibility tests to evaluate their ability for EMI shielding in the radio-frequency range. The performed tests indicated differences in the EMI spectra of ICP-based composites compared to classic CFRP structures. The highest deviation of these spectra was observed in the range of 30–35 MHz. The spectrum of the electromagnetic background radiation for the prototype with the PPy-based CFRP housing was 20 dBµV/m, corresponding to 8 dB of shielding effectiveness (SE) for both ICP-based compounds with respect to the CFRP structures. The obtained values confirm the increasing effectiveness of shielding in the low-frequency interference range typical for motors and power supplies. These results validate the expected ability of EMI shielding in the developed composites, as well as confirm the multifunctionality of the developed materials, which, besides their EMI shielding properties, can conduct electrical current with a conductivity typical for semiconductors, and thus can be used as lightning strike protection materials.

3. Conclusion

Therefore, what we can infer from this is that several variables play a key role in providing better EMI shielding effectiveness. These variables may include material composition, thickness, and method of preparation. In this paper, we shed light on the different shielding effectiveness values for the various materials we have chosen. We observed that reduced graphene oxide works best as a casing over electrical components due to its excellent absorption power; however, this rate of absorption may vary with the material composition. The other two materials are more effective when used for the structural aspects of the drone, each exhibiting different tensile strengths.

4. References

[1] Wikipedia contributors. (n.d.). Unmanned aerial vehicle. In Wikipedia, The Free Encyclopedia. Retrieved September 8, 2024, from **https://en.wikipedia.org/wiki/Unmanned_aerial_vehicle.**

[2] Kubacki, R., Przesmycki, R., & Laskowski, D. (2023). Electronics, 12(18), 3973. **https://www.mdpi.com/2079-9292/12/18/3973.**

[3] Turczyn, R., Krukiewicz, K., Katunin, A., Sroka, J., & Sul, P. (2019). Composites Part B: Engineering, 177, 107425. **https://www.sciencedirect.com/science/article/pii/S0263822319323670.**

[4] Ahmed, I., Jan, R., Khan, A. N., Gul, I. H., Khan, R., Javed, S., Akram, M. A., Shafqat, A., Cheema, H. M., & Ahmad, I. (n.d.). Materials Research Express. **https://iopscience.iop.org/article/10.1088/2053-1591/ab62ed/meta.**

[5] Rashid, I. A., Tariq, A., Shakir, H. M. F., Afzal, A., Ali, F., Abuzar, M., & Haider, T. (n.d.). Journal of Composite Materials. **https://journals.sagepub.com/eprint.**

[6] Zhang, X., Yan, X., Guo, J., Liu, Z., Jiang, D., He, Q., Wei, H., Gu, H. A., Colorado, H. A., Zhang, X., & Guo, Z. (2014). Journal of Materials Chemistry C, 2(44), 9598-9609. **https://pubs.rsc.org/en/content/articlehtml/2014/tc/c4tc01978d**.

[7] Setiadji, S., Nuryadin, B. W., Ramadhan, H., Sundari, C. D. D., Sudiarti, T., Supriadin, A., & Ivansyah, A. L. (2018). IOP Conference Series: Materials Science and Engineering, 434(1), 012079. **https://iopscience.iop.org/article/10.1088/1757-899X/434/1/012079/pdf.**

[8] Setiadji, S., Nuryadin, B. W., Ramadhan, H., Sundari, C. D. D., Sudiarti, T., Supriadin, A., & Ivansyah, A. L. (2015). Advances in Materials Science and Engineering, 2015, 168125. **https://onlinelibrary.wiley.com/doi/pdf/10.1155/2015/168125**.

[9] Kubacki, R., Przesmycki, R., & Laskowski, D. (2023). Electronics, 12(18), 3973. **https://www.mdpi.com/2079-9292/12/18/3973**.

[10] Araz, İ. (n.d.). Turkish Journal of Electrical Engineering & Computer Sciences. **https://journals.tubitak.gov.tr/cgi/viewcontent.cgi?article=1805&context=elektrik.**

[11] Yao, Y., Jin, S., Zou, H., Li, L., Ma, X., Lv, G., Gao, F., Lv, X., & Shu, Q. (2021). Journal of Polymer Research, 28, 75.

5. Conflict of Interest

The author declares no competing conflict of interest.

6. Funding

No funding was received to support this study.